M&C 2017 - International Conference on Mathematics & Computational Methods Applied to Nuclear Science & Engineering, Jeju, Korea, April 16-20, 2017, on USB (2017)

Comparisons of Three Monte Carlo Transport Codes in Cask Shielding Calculations: MCNP, MAVRIC, and ADVANTG/MCNP

Po-Chen Lai[1], Yu-Shiang Huang[1,2], Rong-Jiun Sheu[1,3,*]

[1]*Institute of Nuclear Engineering and Science, National Tsing Hua University, Hsinchu 30013, Taiwan, R.O.C.*
[2]*Nuclear Science and Technology Development Center, National Tsing Hua University, Hsinchu 30013, Taiwan, R.O.C.*
[3]*Department of Engineering and System Science, National Tsing Hua University, Hsinchu 30013, Taiwan, R.O.C.*
E-mail: rjsheu@mx.nthu.edu.tw

Abstract – *This paper presents a detailed comparison of two Monte Carlo codes with different FW-CADIS implementations (MAVRIC and ADVANTG/MCNP) for solving a difficult real-world cask shielding problem. The predicted surface dose rate distributions were compared to each other as well as to a straightforward MCNP calculation for reference. Both MAVRIC and ADVANTG/MCNP achieved substantial improvements in overall computational efficiencies, especially for gamma-ray transport. Compared with the continuous-energy MCNP and ADVANTG/MCNP calculations, the multigroup MAVRIC calculations underestimated the neutron dose rates at the cask side by approximately a factor of 2 and slightly overestimated the gamma-ray dose rates at the cask surfaces.*

I. INTRODUCTION

Radiation shielding analysis for interim dry storage of spent nuclear fuels in Taiwan is a critical issue with regulatory bodies and the public because of a stringent design dose limit and a short distance to the site boundary. During design phase and review process, many shielding analyses and repeated calculations are necessary to optimize and verify the shielding requirements. It involves many computational difficulties, including complicated source and geometry modeling, deep-penetration calculation, radiation streaming through cooling ducts, and skyshine evaluation. The Monte Carlo (MC) method is one of the choices for the task and usually the preferable one because of its powerful capabilities in geometry modeling and calculation accuracy. However, MC simulations could be time-consuming such as the case encountered here. To make a challenging MC simulation computationally practical, effective variance-reduction techniques are indispensable.

Recent development in advanced MC codes has often emphasized the benefits of using deterministic adjoint functions for variance reduction. The Consistent Adjoint Driven Importance Sampling (CADIS) methodology is one of the major achievements in this trend [1,2]. In this study, we adopted MAVRIC [3] and ADVANTG [4] to reexamine a cask shielding problem described in the safety analysis report (SAR) of the independent spent fuel storage installation (ISFSI) at the Kuosheng nuclear power plant in Taiwan. Surface dose rates of the storage cask were of most interest. Both MAVRIC and ADVANTG were developed based on the CADIS methodology. Their results were compared to each other as well as to a straightforward MCNP [5] calculation with mostly default settings. The comparisons among these codes was evaluated in terms of their accuracies in dose rate prediction and computational efficiencies. The comparison results and experience obtained from this work should be useful and helpful to others performing similar shielding analyses.

II. MATERIALS AND METHODS

1. Spent Fuels and Storage Cask

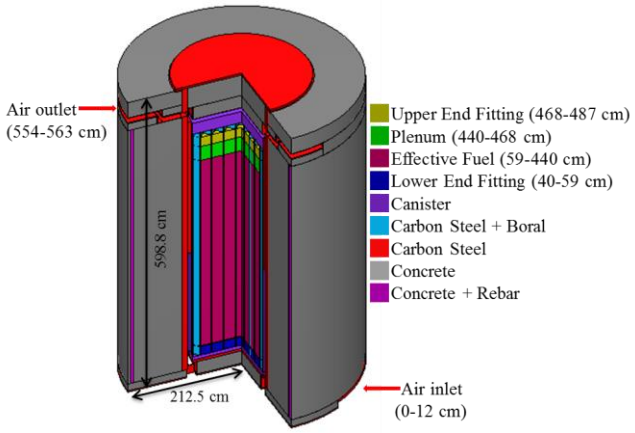

Fig. 1. A cutaway view of the cask geometry model.

The Kuosheng nuclear power plant is the second nuclear power plant in Taiwan and currently the largest one, having 2 units of BWR-6 with a power generation of 2×985 MW_e. It has been commercially operated for more than 35 years. In order to solve the shortage problem of spent fuel storage, Taiwan Power Company proposed an ISFSI facility at the plant site with a maximum capacity of 27 storage casks at phase one for interim dry storage of spent fuels. According to its SAR [6], the storage cask was essentially the MAGNASTOR type of NAC International Inc. [7] with some shielding enhancements to comply with the promised dose limit of 0.05 mSv a year at site boundaries. Fig. 1 shows the geometry model of the cask that has overall dimensions of ~6 m in height and ~4.3 m in diameter. It

includes a detailed model of the canister, which can accommodate 87 BWR spent fuel assemblies. Outside the canister, there are steel liner, concrete shielding, air inlets/outlets, and other fine structures.

The design basis of spent fuel was a typical GE8×8-2 fuel assembly with an initial U-235 enrichment of 2.84 %, maximum burnup of 34 GWD/MTU and cooling for 20 years. Three types of radiation sources were under consideration: fuel neutron (FN), fuel gamma (FG), and hardware gamma (HG). FN and FG sources coming from actinides and fission products in spent fuels were contained only in the effective fuel region. In addition, there were HG sources in the upper end fitting (UEF), plenum, effective fuel, and lower end fitting (LEF) regions, mainly caused by neutron activation in structure materials. TABLE I lists the regional intensities of these sources. Their spatial and energy distributions used in simulations were the same as those adopted in the SAR.

TABLE I. Total source intensities of 87 spent fuels in the MAGNASTOR cask.

Source	Region	Strength (n or γ/s/cask)
FN	Effective fuel	4.813×10^{09}
FG	Effective fuel	6.577×10^{16}
HG	LEF	6.020×10^{13}
	Effective fuel	2.818×10^{13}
	Plenum	3.757×10^{13}
	UEF	1.793×10^{13}

2. Calculation Models

Three MC transport codes were employed to estimate the surface dose rates of the cask illustrated in Fig. 1: MCNP5 version 1.60, the MAVRIC sequence in SCALE version 6.1, and the ADVANTG automated variance reduction generator (version 3.0.3) with MCNP5, abbreviated here as ADVANTG/MCNP. Although MCNP itself is rich in variance reduction features, a straightforward MCNP simulation without user-specified variance reduction techniques was conducted as a reference case for comparison. As indicated in TABLE II, MAVRIC and ADVANTG are hybrid methods based on the CADIS methodology, taking advantage of approximate 3-D multigroup discrete ordinates (S_N) transport solutions provided by Denovo [8]. MAVRIC passed the variance reduction parameters to the designated MC code Monaco, while ADVANTG can be directly used with unmodified versions of MCNP5. One of the key differences between the MAVRIC and ADVANTG/MCNP transport calculations was the format of the underlying cross sections. MCNP can perform continuous-energy MC transport calculations while Monaco in this version only supported multigroup cross sections. Both the continuous-energy cross sections used in MCNP and the 27N19G multigroup cross sections used in Denovo and Monaco [9] were derived from the same version of ENDF/B-VII library.

For a complicated real-world shielding problem such as this case, it is difficult to have a fair performance comparison between different MC codes that are designed for general purpose applications. Nevertheless, we endeavored to make the comparisons in this study as trustworthy as possible by carefully checking the calculation models built by three codes, ensuring they have the same geometry, material, source and detector representations. The forward-weighted CADIS implementation (FW-CADIS) in the MAVRIC and ADVANTG/MCNP simulations requires two separate S_N calculations in forward and adjoint modes [10], respectively. Since only approximate S_N solutions were needed, the spatial discretization of the problem domain was made rather coarse, representing the complicated storage cask in a small number of XYZ meshes (98×98×58). In the adjoint mode calculation, a thin volume source covering the entire cask surface above the ground was defined to guide particles in the subsequent MC simulation to move as outwardly as possible. The FW-CADIS method further helped to produce relatively uniform statistical uncertainties across multiple tallies at the cask surface.

In addition to mesh tallies covering the entire cask, the average dose rate at the cask top surface was scored by a thin circular disk with a radius of 92 cm, the same as the effective fuel region. Similarly, the average dose rate at the side surface was defined by scoring a cylindrical shell with a height of 382 cm that covers the effective fuel region. The two cell tallies were arranged to indicate average dose levels at the cask surfaces and facilitate the comparison of computational efficiencies among various calculations. Dose rates were obtained by folding the calculated neutron and gamma-ray spectra with appropriate fluence-to-dose conversion factors. The computational efficiency was defined using the figure of merit (FOM), which is the inverse of the product of the error squared and the total computing time in minutes.

III. RESULTS AND DISCUSSION

1. Average Dose Rates and Figure of Merits

Considering three MC codes and three different source terms, a total of nine separate fixed-source simulations were necessary to have a complete analysis of dose rate distribution around the cask. The execution time of each simulation was limited to about the same (~1 day) for an intuitive comparison of the resulting statistical uncertainties. All calculations were carried out on a Windows 7 computer equipped with a 3.4 GHz CPU and 16 GB RAM. TABLE III lists the computing time of these simulations, noticing the time spent in various modules of the FW-CADIS runs. The S_N calculations either in forward or adjoint mode took approximately 10-15 minutes for gamma source problems and spent about 1 hour for the fuel neutron cases that

involve neutron/gamma coupled transport. The computing time for a 3-D S_N calculation could be long, mainly depending on the size of spatial discretization and required accuracy of the solution.

TABLE IV compares average surface dose rates at the cask top/side surfaces calculated by MCNP, MAVRIC, and ADVANTG/MCNP. For the FN source case, the straightforward MCNP calculation obtained reasonable estimates in an affordable computing time. The ADVANTG/MCNP results were consistent with MCNP as expected and, more importantly, the variance reduction scheme resulted in overall improvements in computational efficiency, especially for two neutron tallies that yielded approximately two orders of magnitude improvement. The speedup was measured as the FOM ratio between two runs. Also based on the FW-CADIS methodology, MAVRIC in this case generally achieved similar or slightly lower performance in computational efficiency when compared with ADVANTG. However, the MAVRIC calculations underestimated the neutron and gamma-ray dose rates at the cask side surface and overestimated the dose rates at the cask top surface to varying degrees when compared with the MCNP or ADVANTG/MCNP results. The MCNP-related calculations with continuous-energy cross-section data were generally considered more accurate and reliable than those obtained by multigroup calculations, especially for deep-penetration calculations in this case.

The FG source consisted of mostly low-energy gamma rays. The straightforward MCNP calculation in this case recorded nothing at the cask surfaces even after 26 hours of execution time. For the HG source with relatively higher energies, some gamma rays penetrated the cask shielding and reached the surface detectors. But, as shown in TABLE IV, the statistical uncertainties were too large to be meaningful. In contrast, MAVRIC and ADVANTG/MCNP achieved substantial improvements in computational efficiency of gamma-ray transport, especially for two cask side cases as indicated by their large FOMs. Compared with the ADVANTG/MCNP predictions, MAVRIC slightly overestimated the gamma-ray dose rates at the cask surfaces.

2. Dose Rate Distributions at Cask Surfaces

Figs. 2 and 3 show the distributions of neutron, gamma-ray, and total dose rates at the cask side/top surfaces calculated by MCNP, MAVRIC, and ADVANTG/MCNP. The general shapes of their predicted dose rate profiles are similar to each other. Focusing first on neutron dose rates around the cask, the maximal dose rate at the cask side surface occurred near the bottom air inlets and that at the cask top surface appeared around the location of the air gap between the canister and concrete cask. The phenomenon was expected due to the effect of neutron streaming. The statistical uncertainties of three simulations with roughly the same computing time indicated that the computational efficiency of ADVANTG/MCNP was approximately comparable to that of MAVRIC, and these two FW-CADIS simulations significantly surpassed the performance of MCNP without variance reduction R. The MCNP neutron tallies at the cask side, although with large statistical fluctuations, were about consistent with those provided by ADVANTG/MCNP. However, compared with the continuous-energy MCNP calculations, the multigroup MAVRIC calculation underestimated the neutron dose rates at the cask side by approximately a factor of 2. Insufficient self-shielding correction in multigroup neutron cross sections should be the most probable cause of the discrepancy. With the new continuous-energy capabilities introduced in SCALE 6.2, future study using continuous-energy MAVRIC calculations should clarify this issue.

The gamma-ray dose rates at the cask side surface in Fig. 2 show a rather smooth profile and have a broad peak around the middle of the effective fuel region. The streaming of gamma rays along air inlets was not significant as that of neutrons. The dose rate peak at the cask top surface still occurred at the location of the air gap surrounding the canister. Among the comparison of three MC codes, the predicted gamma-ray dose rates at the cask side surface appeared more consistent to each other except at cask heights above 400 cm. At the cask top surface, the MAVRIC-predicted gamma-ray dose rates were slightly higher than the ADVANTG/MCNP results. The gamma-ray dose rate profiles summed from three 1-day straightforward MCNP calculations for the FN, FG, and HG sources were too noisy to be used in meaningful comparisons.

Neutron dose rates around the cask only come from the FN source term. However, all three source terms including FN, FG, and HG contribute to gamma-ray dose rates at the cask surfaces. Figs. 4 and 5 show the gamma-ray dose rate distributions at the cask side and top surfaces, respectively, due to these three source terms. Apparently, secondary gamma rays induced by neutron interactions were the dominant contributor of gamma-ray dose rates at the cask surfaces except two regions: (1) at the cask side surface with heights of ~500 cm due to the strong and high-energy HG sources from the UEF and plenum, (2) at the cask top surface near the location of air gap where the streaming and penetration of the FG and HG sources are important and have comparable contributions. As shown in Figs. 4 and 5, MAVRIC and ADVANTG/MCNP both based the FW-CADIS methodology provide generally consistent gamma-ray dose rate profiles for each of the three source terms, while the 1-day straightforward MCNP calculations in this case failed to have meaningful predictions on the surface dose rates due to FG and HG sources.

IV. CONCLUSIONS

A real-world cask shielding problem involves not only complex source and geometry configurations but also difficult deep-penetration and streaming calculations. The Monte Carlo method is usually a preferable approach for

solving such a problem. However, effective variance reduction techniques are indispensable to obtain statistically converged results within reasonable computing time. This study focused on comparing the performance of two hybrid transport codes, MAVRIC and ADVANTG/MCNP, in calculating the surface dose rate distribution of a MAGNASTOR spent fuel storage cask. Both codes utilized deterministic forward and adjoint solutions generated by Denovo for automatic variance reduction through source biasing and consistent transport biasing. But, they had different FW-CADIS implementations in Monte Carlo simulations: MAVRIC in this version relied on a multigroup Monte Carlo transport code Monaco while ADVANTG was designed to directly couple with unmodified continuous-energy MCNP calculations.

Compared with the straightforward MCNP calculation without explicit settings for variance reduction, the computational efficiencies of both MAVRIC and ADVANTG/MCNP were improved by a factor of several tens or hundreds for neutron transport, and their efficiencies were tremendously increased by more than several orders of magnitude for two cases involving gamma-ray sources. Digging into the details indicated that the computational efficiency of ADVANTG/MCNP was slightly better than that of MAVRIC in this problem. In terms of accuracy in predicting the surface dose rates, the continuous-energy ADVANTG/MCNP calculations were considered to be more reliable than the multigroup transport of MAVRIC, in particular in simulating deep penetration of neutrons in complicated geometry. The new version of MAVRIC in SCALE 6.2.1, allowing use of either multigroup or continuous-energy cross sections, will eliminate this limitation and extend its capability in accurate shielding analyses for similar problems.

ACKNOWLEDGMENTS

This work was supported by the Fuel Cycle and Material Administration of Atomic Energy Council in Taiwan, under contract no. 104FCMA018.

REFERENCES

1. J.C. WAGNER, A. HAGHIGHAT, "Automated Variance Reduction of Monte Carlo Shielding Calculations Using the Discrete Ordinates Adjoint Function," *Nucl. Sci. Eng.*, **128**, 186 (1998).
2. A. HAGHIGHAT, J.C. WAGNER, "Monte Carlo Variance Reduction with Deterministic Importance Functions," *Prog. Nucl. Energy*, **42**, 25 (2003).
3. ORNL, "SCALE: A Modular Code System for Performing Standardized Computer Analyses for Licensing Evaluations," ORNL/TM-2005/39, Version 6.1, Oak Ridge National Laboratory (2011).
4. S.W. MOSHER, A.M. BEVILL, S.R. JOHNSON, A.M. IBRAHIM, C.R. DAILY, T.M. EVANS, J.C. WAGNER, J.O. JOHNSON, R.E. GROVE, "ADVANTG - An Automated Variance Reduction Parameter Generator," ORNL/TM 2013/416 Rev. 1, Oak Ridge National Laboratory (2015).
5. X-5 MONTE CARLO TEAM, "MCNP - Version 5, Vol. I: Overview and Theory," LA-UR-03-1987, Los Alamos National Laboratory report (2003).
6. TPC, "Safety Analysis Report for the ISFSI in Nuclear Power Plant 2," Taiwan Power Company (2012).
7. NAC, "MAGNASTOR (Modular Advanced Generation Nuclear All-purpose STORage) Safety Analysis Report," Docket No. 72-1031, NAC International Inc. (2009).
8. T.M. EVANS, A.S. STAFFORD, R.N. SLAYBAUGH, K.T. CLARNO, "Denovo: A New Three-Dimensional Parallel Discrete Ordinates Code in SCALE," *Nucl. Technol.*, **171**, 171 (2010).
9. M.B. EMMETT, J.C. WAGNER, "Monaco: A New 3D Monte Carlo Shielding Code for SCALE," *Trans. Am. Nucl. Soc.*, **91**, 701 (2004).
10. J.C. WAGNER, D.E. PEPLOW, S.W. MOSHER, "FW-CADIS Method for Global and Semi-Global Variance Reduction of Monte Carlo Radiation Transport Calculations," *Nucl. Sci. Eng.*, **176**, 37 (2014).

TABLE II. Calculation tools, methods, and cross sections used in this study.

Code package	Hybrid method	Cross-section data
MCNP5 (v1.60)	n/a	ENDF/B-VII, continuous-energy
MAVRIC in SCALE (v6.1)	S_N (Denovo) + MC (Monaco)	ENDF/B-VII, multigroup 27N19G (Denovo) + multigroup 27N19G (Monaco)
ADVANTG (v3.0.3) with MCNP5 (v1.60)	S_N (Denovo) + MC (MCNP)	ENDF/B-VII, multigroup 27N19G (Denovo) + continuous-energy (MCNP)

TABLE III. Comparisons of computing time of simulations involving three MC codes and three different source terms.

	Source	Forward S_N (min)	Adjoint S_N (min)	Total S_N (min)	MC (hr)	Total (hr)
MCNP	FN	n/a	n/a	n/a	26.00	26.00
	FG	n/a	n/a	n/a	26.00	26.00
	HG	n/a	n/a	n/a	26.00	26.00
MAVRIC	FN	79.01	50.19	130.63	26.17	28.35
	FG	13.75	12.08	27.23	26.57	27.02
	HG	12.15	12.29	26.07	25.85	26.28
ADVANTG/MCNP	FN	64.46	48.49	115.55	24.09	26.02
	FG	11.68	14.59	27.62	25.55	26.01
	HG	10.21	14.49	25.95	25.59	26.02

TABLE IV. Comparisons of average surface dose rates at the cask top/side surfaces calculated by MCNP, MAVRIC, and ADVANTG/MCNP.

Source	Detector	MCNP			MAVRIC			ADVANTG		
		Dose rate (mSv/h)	Error (%)	FOM (/min)	Dose rate (mSv/h)	Error (%)	FOM (/min)	Dose rate (mSv/h)	Error (%)	FOM (/min)
FN	Side Neutron	3.33×10^{-5}	7.72	0.11	1.80×10^{-5}	0.60	17.50	3.53×10^{-5}	0.52	23.69
	Top Neutron	1.45×10^{-4}	19.84	0.02	2.68×10^{-4}	4.20	0.36	1.91×10^{-4}	2.16	1.37
	Side Gamma	3.20×10^{-4}	0.60	17.80	2.81×10^{-4}	0.65	15	3.22×10^{-4}	0.64	15.64
	Top Gamma	2.09×10^{-4}	4.07	0.39	2.25×10^{-4}	1.49	2.88	2.03×10^{-4}	1.96	1.67
FG	Side Gamma	-	-	-	7.22×10^{-5}	0.12	430	4.99×10^{-5}	0.10	641
	Top Gamma	-	-	-	2.68×10^{-4}	6.00	0.17	2.13×10^{-4}	4.29	0.35
HG	Side Gamma	3.68×10^{-6}	78.23	0.001	1.56×10^{-5}	0.13	396	8.78×10^{-6}	0.11	529
	Top Gamma	2.50×10^{-4}	47.03	0.003	4.89×10^{-4}	1.97	1.65	3.50×10^{-4}	0.99	6.54

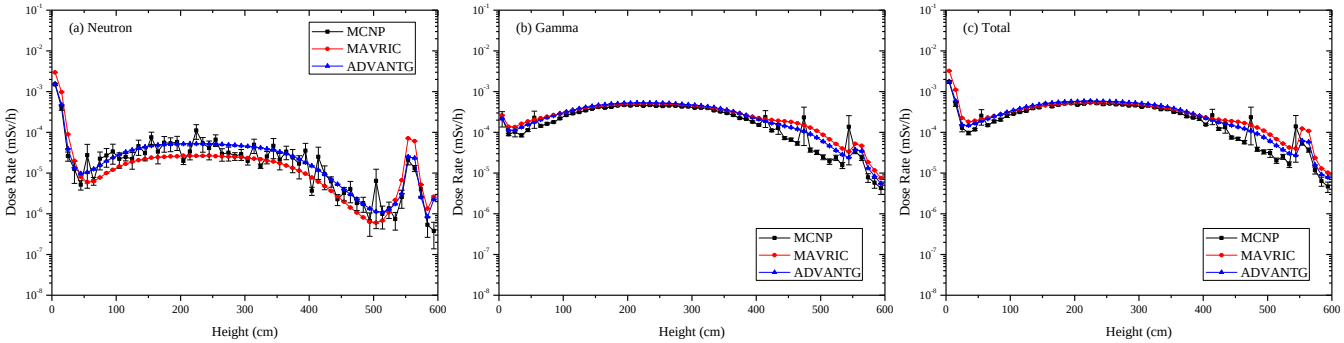

Fig. 2. Comparisons of dose rate distributions (neutron, gamma-ray, and total) at the cask side surface calculated by MCNP, MAVRIC, and ADVANTG/MCNP.

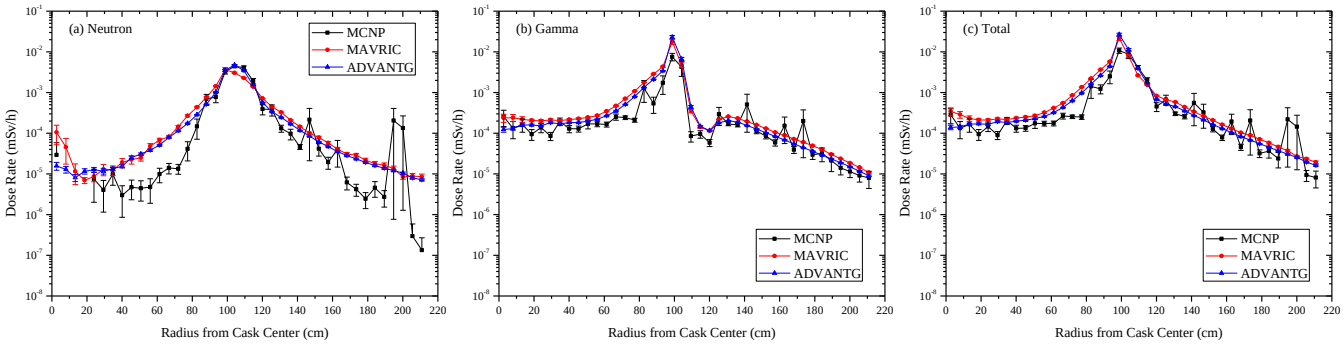

Fig. 3. Comparisons of dose rate distributions (neutron, gamma-ray, and total) at the cask top surface calculated by MCNP, MAVRIC, and ADVANTG/MCNP.

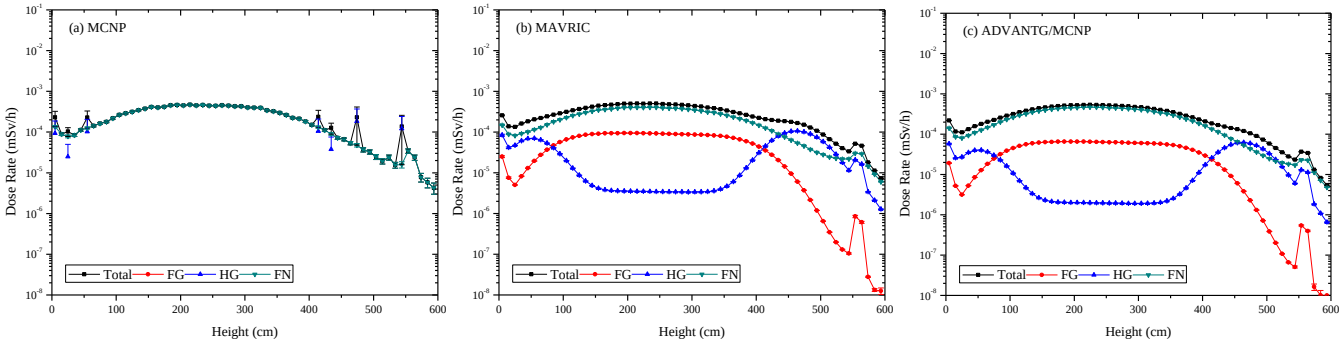

Fig. 4. Gamma-ray dose rate distributions at the cask side surface calculated by MCNP, MAVRIC, and ADVANTG/MCNP due to three source terms (FN, FG, and HG).

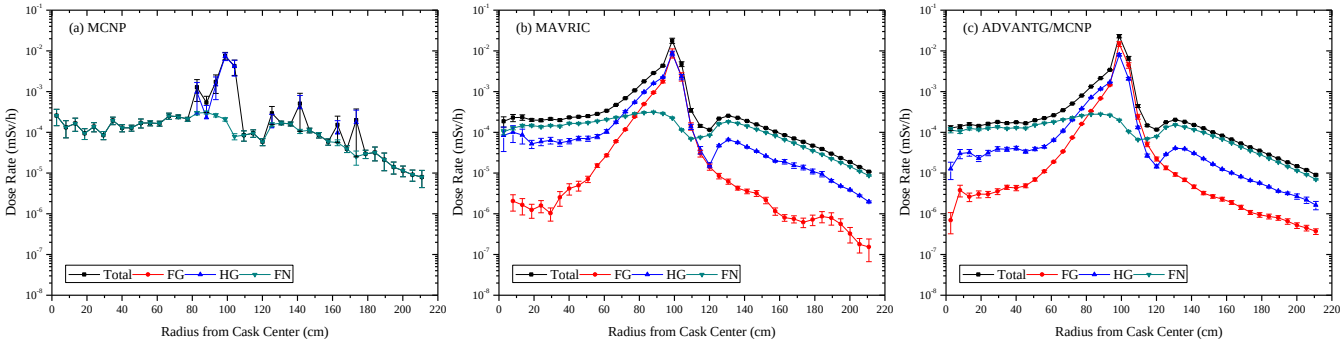

Fig. 5. Gamma-ray dose rate distributions at the cask top surface calculated by MCNP, MAVRIC, and ADVANTG/MCNP due to three source terms (FN, FG, and HG).